Physics of Nuclear Energy Deposition for the Deflection of Asteroids and Comets

Kirsten Howley, Robert Managan & Joseph Wasem

Lawrence Livermore National Laboratory, Livermore, CA, USA

Planetary Defense Conference, Frascati, Italy
April 13-17, 2015

Abstract

Deflection using a stand-off nuclear explosion works by heating surface material such that it is ejected, which provides thrust to the remaining mass. Since the magnitude of the deflection achieved scales with the amount of mass ejected, it is desirable to heat larger masses to a lower temperature rather than smaller masses to a higher temperature. In both cases, energy densities sufficient to melt material must be reached in order to achieve deflection. Here, we explore the effect of neutrons and photons on various asteroid- and comet-like materials.

How Deflection Using a Nuclear Explosion Works

Asteroid and comet deflection using a stand-off nuclear explosion works by heating surface material such that it is ejected, thereby providing thrust to the remaining mass.

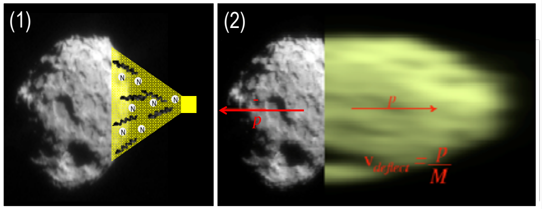

Above: Illustration of how deflection using a nuclear device works. (1) A nuclear device intercepts a body at some standoff distance. The device goes off depositing energy into the object in the form of neutrons and photons. (2) The material heats up and blows off. Because of conservation of momentum, the blow-off imparts momentum to the remaining mass resulting in a deflection event.

Energy Coupling

Using the N-particle transport codes MCNP and Mercury, energy deposition profiles for photons and neutrons are determined as a function of energy type, angle of incidence and target material.

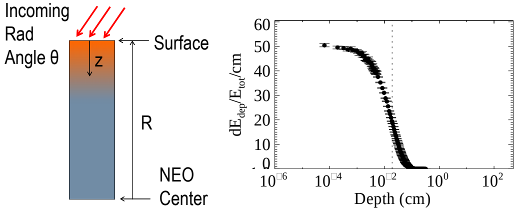

Left: Cartoon illustrating how 1D energy deposition profiles are determined as a function of energy type, material and angle of incidence in MCNP and Mercury. *Right:* Energy deposition profile of a 10 keV source into SiO_2 as a function of depth at normal incidence.

Analytic Approximation

We develop a simple analytic approximation to model how energy couples to a material. We assume that the probability of a mono-energetic photon or neutron interacting within a homogenous material decreases exponentially with path length (Beer-Lambert Law). Using this assumption, we can characterize the energy deposition profile as a function of depth *z*,

$$\boxed{f(z) = \frac{\eta_Y}{\delta} \exp\left[-\frac{z}{\delta}\right]}$$

where the skin depth δ is the depth at which 1-1/e fraction of the energy has been deposited and the yield coupling efficiency η_Y is the fraction of incident energy deposited. The goal of this approximation is to construct analytic deposition equations that can be applied to a variety of 2D and 3D geometries (see posters by Joe Wasem & Rob Managan).

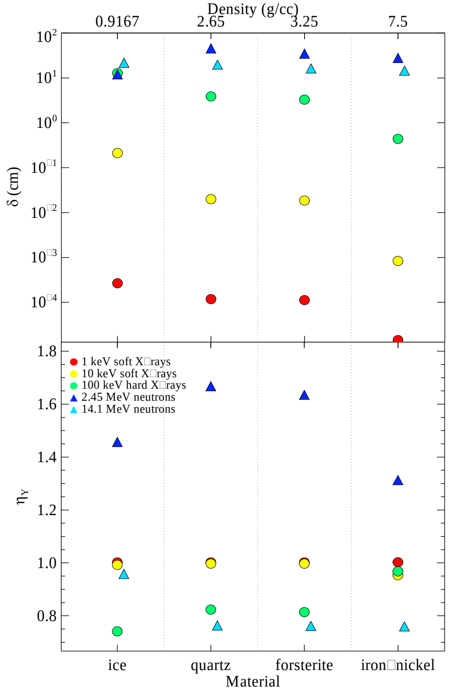

Above: Skin depth δ and yield coupling efficiencies η_Y for photon and neutron sources into different materials determined from MCNP simulations. For all these materials the neutrons penetrate most deeply. Yield coupling efficiencies for the 2.45 MeV neutrons are greater than one due to neutron capture reactions.

Melted/Vaporized Material as a Metric for Deflection

Predicting the response of a particular object is difficult, since ejecta size and velocity distributions rely heavily on the unknown, complicated internal structure of the body. However, lower bounds on the blow-off momentum can be estimated using the melted/vaporized surface material. At identical yields Y_{source} sufficient to melt a given material the blow-off momentum scales as,

$$\boxed{p \propto \sqrt{\delta\, \eta_Y Y_{source}}}$$

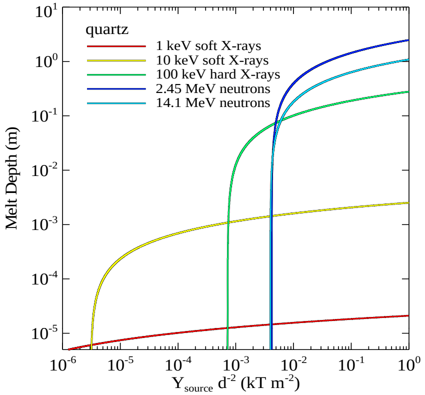

Above: Combining δ and η_Y gives an estimate of the melt depth for different energy sources in SiO_2 as a function of source yield and stand-off distance. The more material melted/vaporized, the larger the push from the initial blow-off.

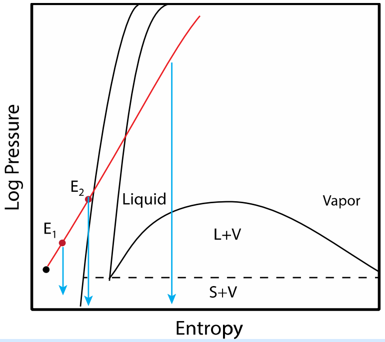

Above: Schematic phase diagram in the pressure-entropy plane illustrating the isentropic expansion of bolide material that has been melted/vaporized as a result of isochoric heating. Material that is melted/vaporized will ultimately be lost from the parent body. Credit: Richard Kraus

LLNL-POST- 669274

This work was performed under the auspices of the U.S. Department of Energy by Lawrence Livermore National Laboratory under Contract DE-AC52-07NA27344, and partially funded by the Laboratory Directed Research and Development Program at LLNL under tracking code 12-ERD-005.